Atomistic mechanism and probability determination of the cutting of Guinier-Preston zones by edge dislocations in dilute Al-Cu alloys

Bin Wu, Zhitong Bai, Amit Misra, and Yue Fan

Phys. Rev. Materials **4**, 020601 — Published 18 February 2020

DOI: 10.1103/PhysRevMaterials.4.020601

Atomistic Mechanism and Probability Determination of the Cutting of GP Zones by Edge Dislocations in Dilute Al-Cu Alloys

Bin Wu[1]*, Zhitong Bai[2], Amit Misra[3], Yue Fan[2]*

1, Key Laboratory of Beam Technology of Ministry of Education, College of Nuclear Science and Technology, Beijing Normal University, Beijing 100875, China

2, Department of Mechanical Engineering, University of Michigan, Ann Arbor, Michigan 48109, U.S.A.

3, Department of Materials Science and Engineering, University of Michigan, Ann Arbor, Michigan 48109, U.S.A.

Abstract:

The interaction between a ½$[\bar{1}10]$(111) edge dislocation and a (001) Guinier-Preston (GP) zone in dilute Al-Cu alloys is studied via atomistic modeling. In stark contrast to the previously reported Orowan looping mechanism where the GP zone remains intact after yield, we discover a new competing mechanism where the dislocation cuts the GP zone into two pieces. We identify the key atomic process triggering the cutting mechanism and calculate its activation barrier at various strains. In further conjunction with the transition state theory, the occurrence probability of the trigger event is mapped out over a broad range of T—$\dot{\varepsilon}$ parameter space. The predictions of the so-constructed mechanism map are validated by parallel MD simulations. The implications of our findings regarding the discrepancies between existing age hardening model and experiments are also discussed.

Corresponding Authors: Bin Wu (bwu6@bnu.edu.cn)
Yue Fan (fanyue@umich.edu)

The superior strength-to-weight ratio endows Al alloys with great potential to be used in aerospace [1, 2], automotive [3], and defense [4] applications. The mechanical performance of Al alloys are largely dictated by the interactions between dislocations and precipitates introduced into the Al matrix, *e.g.* Cu, Mg, Zn, *etc* [5, 6]. To be more specific, the precipitates could impede the dislocations' glide motion in slip planes and thereby enhance the system's flow stress. The degree to which these hardening behaviors are influenced depends on the samples' heat treatment and processing history, because the precipitates' morphology evolution, spatial distribution, and coherency variation with respect to the matrix are all dependent on the applied thermo-mechanical conditions [7]. Therefore, a fundamental knowledge on the dislocation-precipitate interaction under various environments is of crucial importance to develop Al alloys with desired properties.

In Al alloys with supersaturated solid solution of Cu atoms, there is a consensus that the sequence of precipitates evolution is: Guinier-Preston (GP) zone, metastable θ'' and θ' precipitates, and finally the equilibrium θ phases [8]. In the present study we restrict our scope to dislocation-GP zone interaction because, as the very initial stage of the precipitation sequence, GP zone plays a critical role in determining the system's overall age hardening performance. A representative GP zone in Al-Cu alloys is composed of a Cu-concentrated single-layer disc with radius of 1~10 *nm* coherently formed on the {1 0 0} planes [9]. Because of the GP zones' small sizes and their high level coherency with the Al matrix, it is quite challenging to experimentally characterize the detailed mechanism of dislocation-GP zone interaction [10]. Instead, atomistic simulations have been widely employed to tackle such problems [11-15]. According to the conventional wisdom, a small coherent precipitate should be cut by the gliding dislocation. However, a number of atomistic simulations show a distinct Orowan looping mechanism could take place [11-13, 15, 16] or even dominate at certain temperatures and/or GP zone orientations [11, 13]. In other words, a self-consistent and quantitative characterization of dislocation-GP zone interaction yet remains elusive.

Herein we investigate the interaction between a ½$[\bar{1}10](111)$ edge dislocation and a GP zone on the (0 0 1) plane under various thermo-mechanical conditions. In contrast to the reported Orowan looping interaction, the GP zone is also observed to be cut by the glide dislocation. By quantifying the non-linear coupling effect between strain rate and temperature using transition state theory, the probability of occurrence of the cutting mechanism is predicted over a broad range of parameter space. We demonstrate that, at experimental conditions, the cutting mechanism is overwhelmingly more probable than the Orowan looping mechanism. This leads to a reduction of GP zone's growth rate, which provides a natural and viable explanation to the discrepancies between existing model and experimental measurements. The so-constructed probability map, in conjunction with the established multi-scale modeling framework, might improve the physical fidelity of predicting Al-alloys' microstructural evolution and mechanical performance at prescribed conditions.

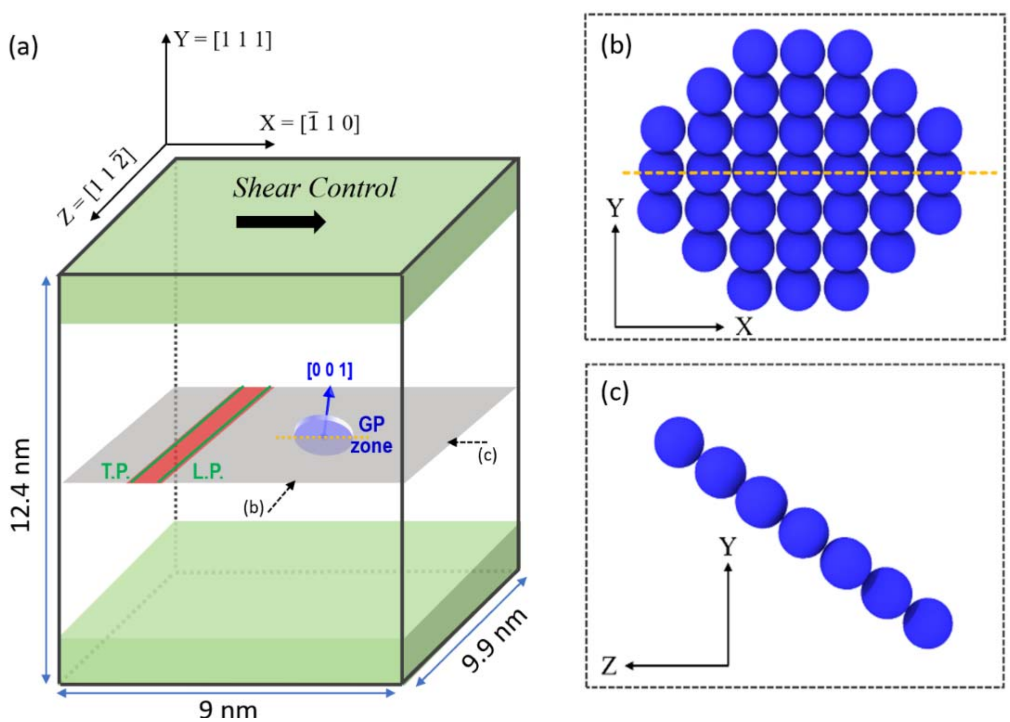

Figure 1 Illustration of simulation setup. The simulation cell in (a) contains 68003 Al atoms and 37 Cu atoms. The edge dislocation consisted of two Shockley partials (green lines) and the center of GP zone composed of Cu atoms (blue disk) are positioned on the central plane (gray). The yellow dashed line represents the section line between

GP zone and glide planes. The projections of GP zone along z and x directions are shown in panels (b) and (c). The atomic configuration is visualized using OVITO [17].

The setup of the model system is illustrated in **Fig. 1**. A ½$[\bar{1}10](111)$ edge dislocation in Al matrix is generated following the periodic array protocol [18, 19]. Due to the low stacking fault energy in FCC metals, the dislocation dissociates into two Shockley partials—a leading partial (L.P.) and a trailing partial (T.P.)— with a separation around 1.1 nm in the slip plane. The GP zone is created as a single-layered disc [10-12] by replacing 37 Al atoms with Cu atoms on the (001) plane. Because the dislocation's Burgers vector is parallel to the section line between the slip and GP zone planes (dashed yellow line in **Fig. 1**), such setup is commonly referred as 0^{o} intersection, as opposed to the 60^{o} scenario where the GP zone is formed on either (0 1 0) or (1 0 0) plane [11-13]. In the present study we restrict our scope to the zero-offset scenario, where the GP zone's center is placed on the dislocation slip plane. A realistic angular-dependent EAM potential for Al-Cu alloy [9] is employed for the present study. Note that a handful of interatomic potentials are available for Al-Cu systems, yet many of them were developed for different aims, such as grain boundary diffusion and amorphous structure. In contrast, the hereby chosen potential was specifically developed to model age hardening process for Al-Cu alloys. Throughout its development, the available experimental and first principle calculation data on lattice parameters, formation energies, and elastic constants of the θ, θ', and some metastable phases were chosen for optimization. Periodic boundary conditions are applied to x and z directions. Two thick blocks of Al atoms on the top and bottom boundaries in y direction are set as rigid bodies. The shear control is enabled by moving the top block with respect to the bottom block at a constant speed v, and the corresponding strain rate is thus given by $\dot{\varepsilon} = v/l_y$, where l_y is the system's dimension in y-axis. The shear stress is calculated as F_t/A_t, where F_t is the total force exerted on the upper block along the Burgers vector direction and A_t is the surface area of the top block.

Fig. 2 shows the stress-strain curves and a few associated atomic configurations at a typical

MD timescale (*i.e.* $\dot{\varepsilon}=10^7\ s^{-1}$) while at different temperatures. In both cases, the dislocation almost instantaneously starts to glide (config. #0 → config. #1) soon as the shear loading is applied, because such slip system's Peierls stress is negligibly small. The L.P. intersects the front edge of GP-zone at the strain around 0.004, causing a small stress drop/relaxation due to the rearrangement of Al atoms along the L.P.. Upon further loading, a precipitate hardening process takes place as the dislocation is pinned to and bowed by the GP zone (configs. #2 & #4), which consequently leads to a rapid increase of shear stress. In spite of such commonality, it is observed that temperature can tremendously affect the dislocation-GP zone interaction, leading to two qualitatively distinct mechanisms as depicted in configs. #3 and #5. More specifically, under the low temperature condition (T=100K) the GP-zone remains almost intact but slightly tilted towards the loading direction after yield. This is consistent with the reported Orowan looping mechanism in the earlier athermal MD simulations [11]. On the other hand, however, under the high temperature scenario (T=600K) the GP zone is cut into two pieces by the dislocation, and the bottom and top halves are shifted against each other by one lattice spacing. It is worth noting that the hereby reported key features of the stress-strain curves and associated interaction mechanisms at low and high temperatures are not sensitive to the initial distance between GP-zone and the leading edge of the dislocation before the onset of loading, which are confirmed by complementary simulations under exactly the same settings except the initial distance being doubled (not shown here).

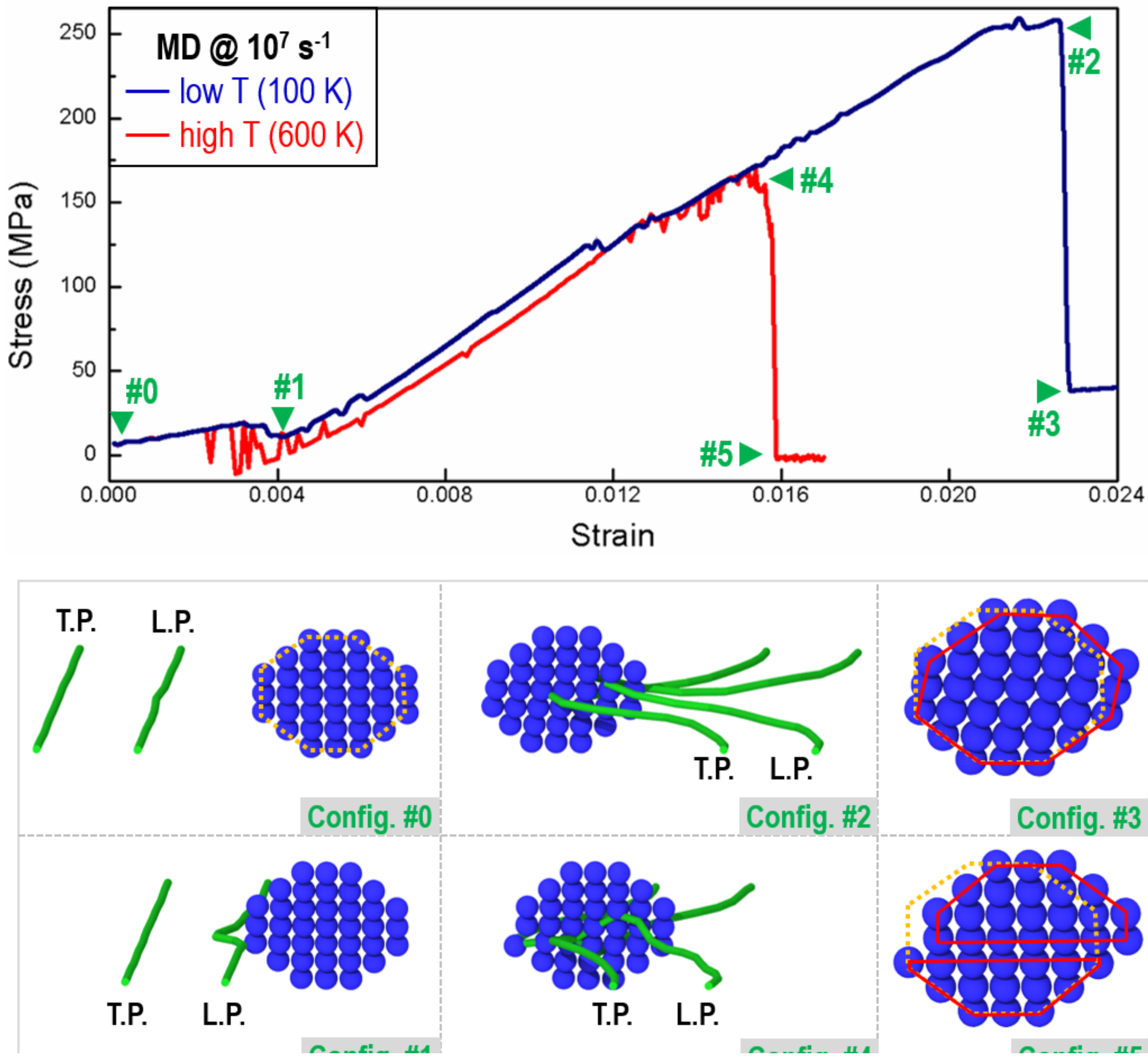

Figure 2: Stress-strain curves and associated atomic configurations at temperatures of 100 K, and 600 K, respectively. The strain rate is kept constant at 10^7/s.

To unravel the underlying physical process of the new cutting mechanism, we first examine the configurational evolution of GP zone at 600K near the yield. The relevant states that facilitate the transformation are illustrated in **Fig. 3**, where the strain ranges from 0.01534 in panel (a) to 0.01584 in panel (f). The key Cu atoms undergoing transition are highlighted by circled numbers.

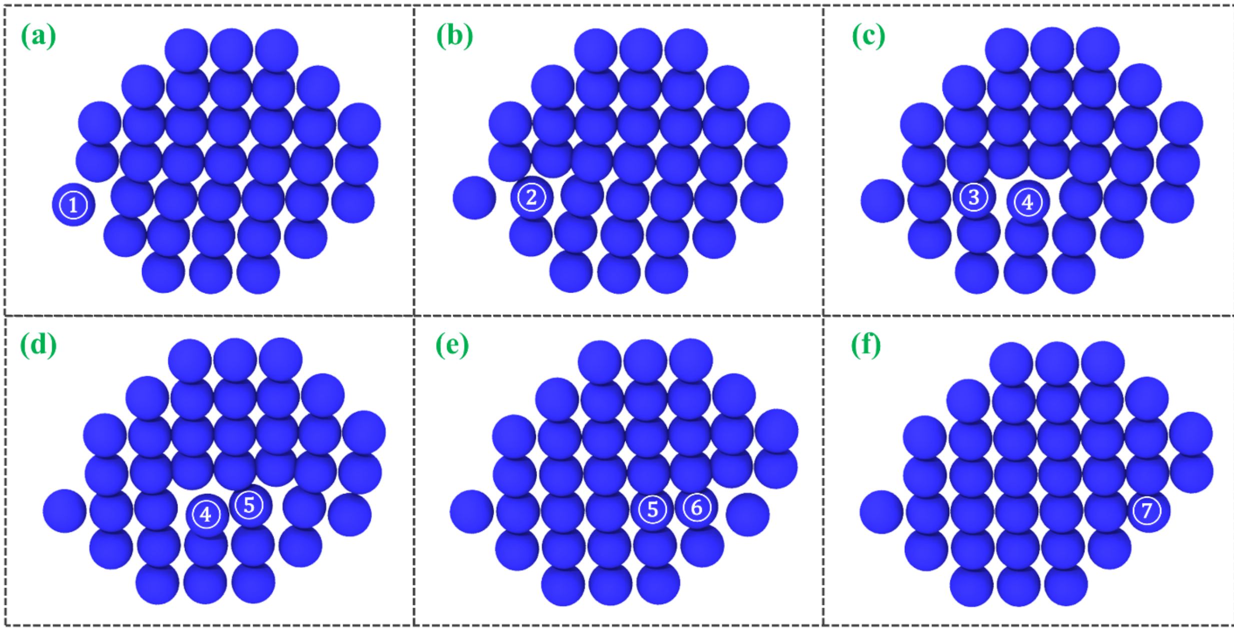

Figure 3 Transformation of GP zone at temperature of 600 K and strain rate of 10^7/s. The strain ranges from 0.01534 in panel (a) to 0.01584 in panel (f). The circled numbers highlight the key Cu atoms undergoing transition to new configuration.

It can be seen that the cutting process consists of a series of sequential steps, where each Cu atom right underneath the slip plane migrates one after another in the direction opposite to loading. It is found that once the migration of first Cu atom (**tag ①**) is initiated, the succeeding Cu atoms will likely follow, and the system will reach its yield point right after. Therefore, the migration of first Cu atom can be considered as the key trigger event for cutting mechanism. In other words, if such trigger event is successfully activated, then it is highly probable that the 0^o GP zone will be cut by the dislocation. By contrast, if the trigger event is not activated then the interaction will likely follow a conventional Orowan looping mechanism, and the GP-zone will remain intact. The significant structural change to the GP zone imparted by the cutting mechanism could affect the kinetics of the GP zone's growth into θ precipitate, which would in turn impact the age hardening behavior of the Al alloys. Therefore, it is of great importance to identify the conditions under which the trigger event can be successfully activated.

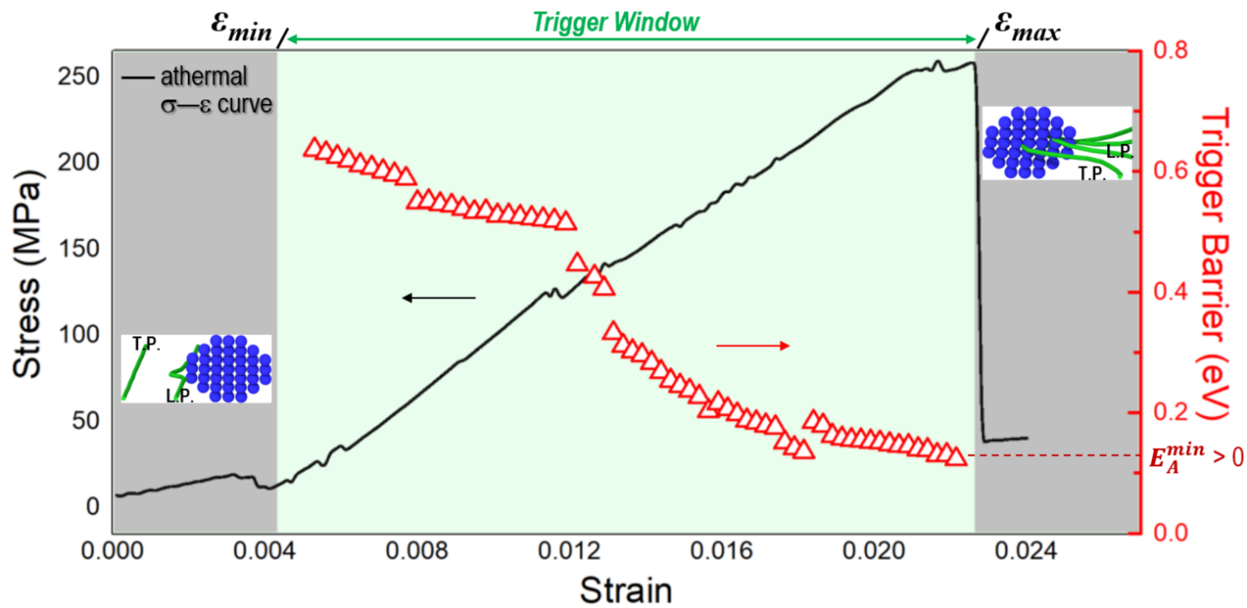

Figure 4 The reaction window where the trigger event could possibly happen and the dependence of its activation barrier on the strain state.

According to transition state theory (TST), the occurrence probability of a thermally activated event is determined by its activation barrier. Hence, we calculate the minimum energy required to enable the first Cu atom (tag ①) in the intact GP-zone under various strain conditions (initial states) to migrate for a significant distance so that the resultant GP-zone structure is the same as that from Fig. 3 (a) (final states) via nudged elastic band (NEB) technique [20, 21]. The results are shown in Fig. 4. Strictly speaking, the initial and final configurations behind each NEB data point are not identical as slight distortion/tilt would occur owing to the distinct macroscopic strain levels. Nevertheless, therein the topological transitions, namely the trigger event depicted in Fig. 3(a), are the same. Two remarkable features are observed: (i) Such event could only occur in a finite window between ε_{min}, where the L.P. just intersects with the GP-zone, and ε_{max}, where the T.P. deeply penetrates into the GP zone and the L.P. already starts to leave. This is because before ε_{min} the dislocation and GP zone are not yet in contact with each other and the GP zone would prefer to stay in a compact structure to minimize its energy; whereas beyond ε_{max} the dislocation will simply pass through the GP-zone following a conventional Orowan looping mechanism; (ii) Within the reaction window the trigger event's activation barrier (E_A) shows a strong dependence on the strain level: E_A is about 0.64 eV at the beginning of interaction and gradually decreases as strain builds up. However, importantly, E_A never drops to zero and the minimum value is 0.12 eV. Such a nonvanishing feature indicates that the trigger event cannot spontaneously happen merely due to the shear loading, and the thermal activation must play a vital role.

These two features make the occurrence probability of the trigger event strongly coupled to the surrounding thermo-mechanical environment. On the one hand, the trigger event should have a larger success probability at a higher temperature. On the other hand, if the applied strain rate ($\dot{\varepsilon}$) is very high, then the duration of the system staying in the reaction window might become too short for the thermal activation to take place. The ultimate success probability is therefore subject to the competition between these two factors, and we seek TST to quantify such interplay. Note that under a strain rate-control scenario, E_A is time-sensitive due to its strong dependence on strain. This makes the classical TST inapplicable [22], and a non-linear coupling effect between $\dot{\varepsilon}$ and T must be considered. The overall success probability of the trigger event at prescribed ($\dot{\varepsilon}$, T) condition can be derived as [23]:

$$P_{trigger}(T,\dot{\varepsilon}) = \frac{1}{\dot{\varepsilon}}\int_{\varepsilon_{min}}^{\varepsilon_{max}} k(\varepsilon)\exp\left[-\frac{1}{\dot{\varepsilon}}\int_{\varepsilon_{min}}^{\varepsilon} k(\varepsilon')d\varepsilon'\right]d\varepsilon, \tag{1}$$

where $k(\varepsilon) = \nu_0\exp\left[-E_A(\varepsilon)/k_BT\right]$, and ε_{min} and ε_{max} represent the lower and upper bound of the trigger reaction window. The attempt frequency ν_0 might vary over a broad range [24, 25], but it should be typically around the order of Debye frequency 10^{12}~10^{13}/s [26-31]. Here we adopt the value of $5*10^{12}$/s as a first order approximation. It is important to point out that this integration shall not depend on the initial spacing between GP-zone and dislocation, because, as noted earlier, the whole reaction window enclosed by ε_{min} and ε_{max} will be collectively translated by the same amount if different initial spacing condition were applied.

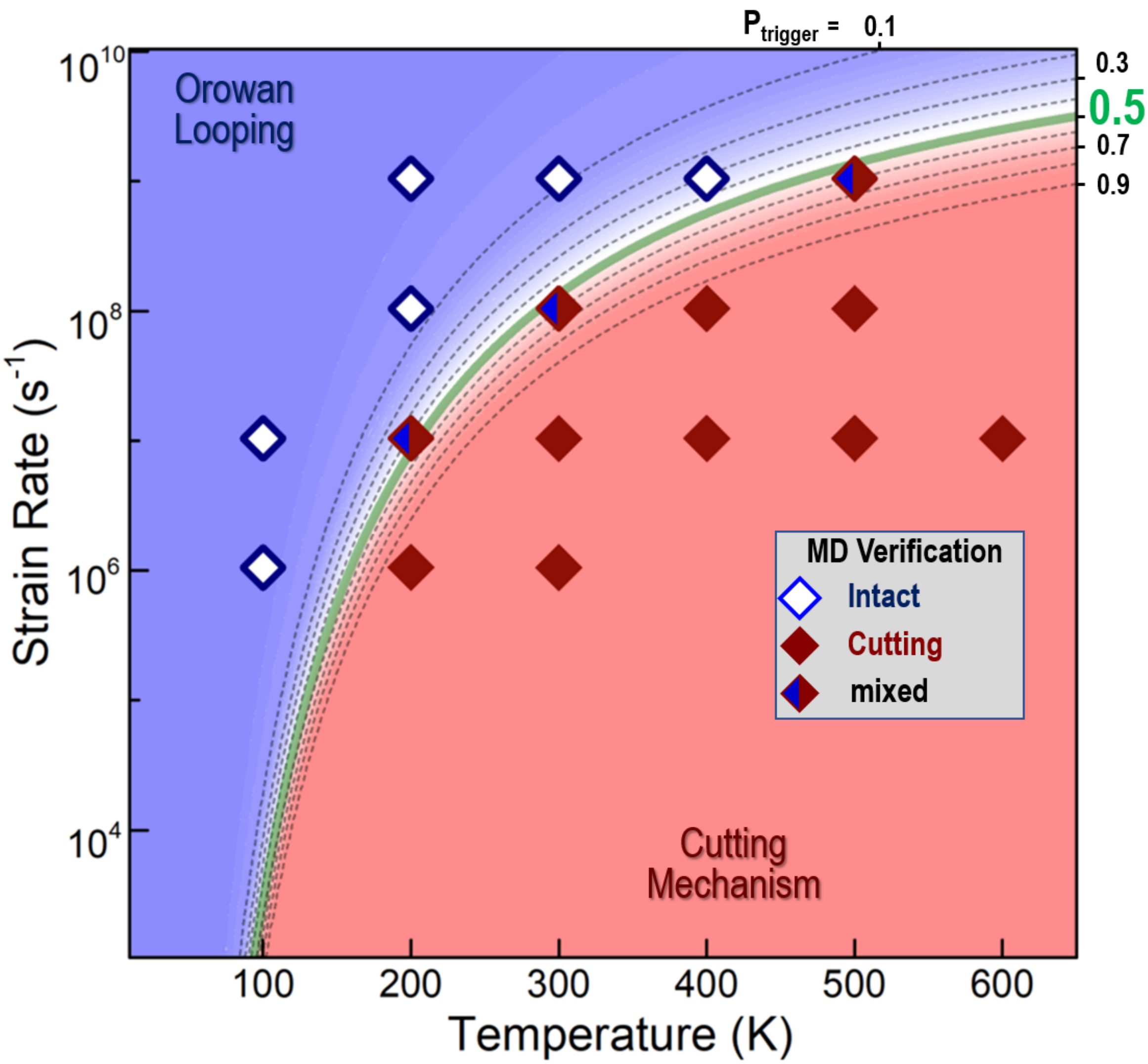

Figure 5 Probability plot of trigger event in the space of strain rate and temperature. Results from MD simulations are superimposed as colored squares. See legends for their meanings.

Eq. (1) allows one to map out the trigger probability in the $\dot{\varepsilon}$—T parameter space. Note that such formulation is derived from TST framework and hence is not limited by the short MD timescales. As marked by the contour lines in **Fig. 5**, $P_{trigger}$ is much smaller in the up-left regime than that in the down-right regime. The $P_{trigger} = 0.5$ curve thus divides the so-constructed map into two qualitatively different regimes, where the Orowan looping and the cutting mechanism are expected to dominate, respectively. To validate such prediction, more independent MD simulations are employed at various thermo-mechanical conditions. The obtained MD results are superimposed in **Fig. 5** as colored squares: blue open squares represent that the GP zone remains intact, while red solid squares correspond to the cutting of GP zone. It is also observed that, for some cases (*e.g.* the half-filled squares) the trigger event is successfully activated, but the GP-zone's cut is not as neat as that in those red solid squares. Hence, we refer such cases as a mixed mechanism. The results of parallel MD simulations are reasonably well consistent with predictions of Eq. (1), suggesting that the hereby considered arguments of coupled $\dot{\varepsilon}$ and T effects are quantitatively accurate. In what follows, we discuss the implications of this mechanism map in the context of age hardening and explain how it can potentially address the discrepancy between existing modeling and experiments.

Earlier atomistic simulations [11, 32, 33] only suggest a single pathway between the 0^{o} GP zone and edge dislocation interaction, namely the Orowan looping mechanism where the GP zone's structure remains intact. Consequently in a multi-scale modeling framework [32, 33], the sizes of GP zones and other precipitates are assumed to increase monotonically via the absorption of solute Cu atoms in the matrix following a classical kinetic growth theory [33-35]. While such a multi-scale methodology can provide valuable insights into understanding the big picture of ageing-induced hardness variation, there are also noticeable discrepancies from experiments on the early stage strengthening and on the width of plateau in the standard ageing curve [32, 33]. It has been argued that the discrepancies can be remedied by artificially suppressing the GP zone's growth, although the underlying physics remains unclear.

According to **Fig. 5**, the newly discovered cutting mechanism is overwhelmingly more likely to happen than the Orowan looping at experimental conditions (*e.g.* $\dot{\varepsilon} < 10^{0} s^{-1}$, $T > 300K$). It can break the GP zone in parts, which naturally slows down the GP zone's growth. In light of such newly imparted mechanism, the kinetic model of GP zone's growth should then consist of two terms, namely a conventional positive term due to the absorption of solute Cu atoms in the matrix, and a negative term accounting for the cutting process by dislocation, respectively. The positive term itself is known dependent on the Cu concentration, and higher concentration of solute Cu atoms will accelerate the growth of GP zone [33, 34]; while the negative term is not explicitly dependent on the Cu concentration because it only concerns the unit interaction between dislocation and individual GP zone. Therefore, the relative importance of the negative term will be enhanced when the concentration of Cu becomes lower. This is in line with the fact that the current multi-scale modeling predictions show larger discrepancies from experiments at decreased Cu concentrations [32].

To summarize, the interaction between an edge dislocation and a GP zone in dilute Al-Cu alloys under 0^{o} intersection condition is investigated via atomistic simulation. In addition to the previously reported Orowan looping mechanism, a distinct new cutting mechanism is discovered. By identifying the governing trigger event leading to such cutting mechanism, quantifying its activation barrier at different strain stages, and considering the non-linear coupling effect between strain rate and temperature, we are able to predict the occurrence probability of the trigger event under a broad range of thermo-mechanical conditions. It is demonstrated that at experimental conditions the newly observed cutting mechanism prevails over the Orowan looping mechanism. This could naturally slow down the growth rate of GP zone and thus provide a viable explanation to the discrepancies between measurements and the existing multi-scale modeling. We therefore see considerable potential of the so-constructed mechanism map in **Fig. 5**, because it can quantitatively delineate the joint effects of temperature and strain rate and thus provide a more comprehensive picture on the dislocation-GP zone interaction beyond the current knowledge. Admittedly, in addition to the strain rate and temperature effects probed in the present study, many other factors (*e.g.* GP zones' sizes and thicknesses, non-zero offset, *etc*) could influence the interaction mechanisms as well. Also, for different loading conditions (e.g. stress control) the dynamic waves may also considerably affect the dislocation's behavior [36]. All these would warrant further studies in the future.

Acknowledgement: This work is supported by the U. S. Army Research Office under Grant No. W911NF-18-1-0119.

Reference:

[1] J. C. Williams and E. A. Starke, Acta Materialia 51 (2003) 5775.
[2] T. Dursun and C. Soutis, Materials & Design (1980-2015) 56 (2014) 862.
[3] W. S. Miller, L. Zhuang, J. Bottema, A. J. Wittebrood, P. De Smet, A. Haszler, and A. Vieregge, Materials Science and Engineering: A 280 (2000) 37.
[4] W. M. Lee and M. A. Zikry, Metallurgical and Materials Transactions A 42 (2011) 1215.
[5] J. E. Hatch and M. American Society for, Aluminum : properties and physical metallurgy, ASM International, Metals Park, OH, 1984.
[6] A. International Conference on Aluminum, J. Hirsch, B. Skrotzki, G. Gottstein, and M. Deutsche Gesellschaft für, Wiley-VCH, Weinheim.
[7] H. Sehitoglu, T. Foglesong, and H. J. Maier, Metallurgical and Materials Transactions A 36 (2005) 749.
[8] Y. Chen, Z. Zhang, Z. Chen, A. Tsalanidis, M. Weyland, S. Findlay, L. J. Allen, J. Li, N. V. Medhekar, and L. Bourgeois, Acta Materialia 125 (2017) 340.
[9] F. Apostol and Y. Mishin, Physical Review B 83 (2011) 054116.
[10] T. E. M. Staab, B. Klobes, I. Kohlbach, B. Korff, M. Haaks, E. Dudzik, and K. Maier, Journal of Physics: Conference Series 265 (2011) 012018.
[11] C. V. Singh and D. H. Warner, Acta Materialia 58 (2010) 5797.
[12] G. Esteban-Manzanares, E. Martínez, J. Segurado, L. Capolungo, and J. Llorca, Acta Materialia 162 (2019) 189.
[13] W. Verestek, A.-P. Prskalo, M. Hummel, P. Binkele, and S. Schmauder, Physical Mesomechanics 20 (2017) 291.
[14] I. A. Bryukhanov and A. V. Larin, Journal of Applied Physics 120 (2016) 235106.
[15] V. S. Krasnikov, A. E. Mayer, V. V. Pogorelko, F. T. Latypov, and A. A. Ebel, International Journal of Plasticity (in press) (2019)
[16] C. V. Singh, A. J. Mateos, and D. H. Warner, Scripta Materialia 64 (2011) 398.
[17] A. Stukowski, Modelling and Simulation in Materials Science and Engineering 18 (2009) 015012.
[18] Y. N. Osetsky and D. J. Bacon, Modelling and Simulation in Materials Science and Engineering 11 (2003) 427.
[19] D. J. Bacon, Y. N. Osetsky, and D. Rodney, in Dislocations in Solids, Vol. Volume 15 (J. P. Hirth and L. Kubin, eds.), Elsevier, 2009, p. 1.
[20] G. Henkelman and H. Jonsson, The Journal of Chemical Physics 113 (2000) 9978.
[21] G. Henkelman, B. P. Uberuaga, and H. Jónsson, The Journal of Chemical Physics 113 (2000) 9901.
[22] Y. Fan, Y. N. Osetsky, S. Yip, and B. Yildiz, Physical Review Letters 109 (2012) 135503.
[23] Y. Fan, Y. N. Osetskiy, S. Yip, and B. Yildiz, Proceedings of the National Academy of Sciences 110 (2013) 17756.
[24] L. Proville, D. Rodney, and M.-C. Marinica, Nat Mater 11 (2012) 845.
[25] P. Koziatek, J.-L. Barrat, P. Derlet, and D. Rodney, Physical Review B 87 (2013) 224105.
[26] G. H. Vineyard, Journal of Physics and Chemistry of Solids 3 (1957) 121.
[27] P. Hänggi, P. Talkner, and M. Borkovec, Reviews of Modern Physics 62 (1990) 251.
[28] Z. Bai and Y. Fan, Physical Review Letters 120 (2018) 125504.

[29] A. F. Voter, F. Montalenti, and T. C. Germann, Annual Review of Materials Research 32 (2002) 321.
[30] Y. Fan, B. Yildiz, and S. Yip, Soft Matter 9 (2013) 9511.
[31] X.-Z. Tang, Y.-F. Guo, Y. Fan, S. Yip, and B. Yildiz, Acta Materialia 105 (2016) 147.
[32] C. V. Singh, in Multiscale Materials Modeling : Approaches to Full Multiscaling (S. Schmauder and I. Schäfer, eds.), De Gruyter, 2016, p. 37.
[33] C. V. Singh and D. H. Warner, Metallurgical and Materials Transactions A 44 (2013) 2625.
[34] M. J. Starink, N. Gao, L. Davin, J. Yan, and A. Cerezo, Philosophical Magazine 85 (2005) 1395.
[35] J. W. Christian, Pergamon, Oxford; Boston, 2002.
[36] J. Cho, J.-F. Molinari, and G. Anciaux, International Journal of Plasticity 90 (2017) 66.